Competing supersolids of Bose-Bose mixtures in a triangular lattice

F. Trousselet, P. Rueda-Fonseca, A. Ralko

Competing supersolids of Bose-Bose mixtures in a triangular lattice

Fabien Trousselet,[1] Pamela Rueda-Fonseca,[2] and Arnaud Ralko[1]

[1]*Institut Néel, Université Grenoble Alpes and CNRS, F-38042 Grenoble, France*
[2]*CEA, INAC-SP2M, F-38054 Grenoble, France*

(Dated: February 6, 2014)

We study the ground state properties of a frustrated two-species mixture of hard-core bosons on a triangular lattice, as a function of tunable amplitudes for tunnelling and interactions. By combining three different methods, a self-consistent cluster mean-field, exact diagonalizations and effective theories, we unravel a very rich and complex phase diagram. More specifically, we discuss the existence of three original mixture supersolids: (i) a commensurate with frozen densities and supersolidity in spin degrees of freedom, in a regime of strong interspecies interactions; and (ii) when this interaction is weaker, two mutually competing incommensurate supersolids. Finally, we show how these phases can be stabilized by a quantum fluctuation enhancement of peculiar insulating parent states.

I. INTRODUCTION

In nowadays condensed matter physics, common fascinating collective behaviors and novel quantum phases are reported in various domains of physics, more specifically in bosonic systems encountered in quantum magnetism, ultracold atoms on optical lattices and strongly correlated materials. Thanks to their versatility, an important amount of exotic phases has been reported in the literature these last years, both experimental and theoretical, such as different types of superfluids[1], insulators[2,3], Bose metals[4–6] or supersolid phases[7–12]. In the latter, the system enters a phase combining crystalline order and superfluidity, and typically arising from the quantum melting of a Mott insulator; this phenomenon is at the origin of intense scientific activities and debates; Experimentally, indications for supersolidity were supposed to be found in ^{4}He[8]. However, necessary conditions for continuous symmetry breaking questioned this interpretation[9] and recent experiments have clearly ruled out this scenario[14].

Meanwhile, supersolids are easier achieved on lattice systems; whereas on a square geometry with nearest neighbor interactions a soft-core description is required[15], they can also be found in hard-core bosonic models when frustration is induced by either further neighbor interactions[10] and/or lattice geometry, *e.g.* triangular[11–13]. An other interesting direction to stabilize supersolidity is to increase the number of degrees of freedom in frustrated systems. In that respect, bosonic mixtures with several species of bosons, usually encountered in optical lattices[16,17], either heteronuclear[18] or homonuclear[19], as well as bilayer systems with interactions but no hopping between layers[20] are very promising. Such systems allow for an even broader variety of quantum phases than their single-species counterparts, depending on the intra- and inter-species interactions, and on the dimension and lattice connectivity.

Theoretically, compared to an already rich literature on mixtures in 1D[21] only few works have focused on 2D cases for instance on square[22] and triangular[23–25] lattices. In all those systems, when contact and dipolar interactions[20,26,27] are taken independently, interaction-induced insulators, *e.g.* density-homogeneous or density wave[28,29] are favored. Hence, their competition can, along with quantum fluctuations, trigger various unconventional phases[11,20,27,30], especially in systems with kinetic or interaction frustration.

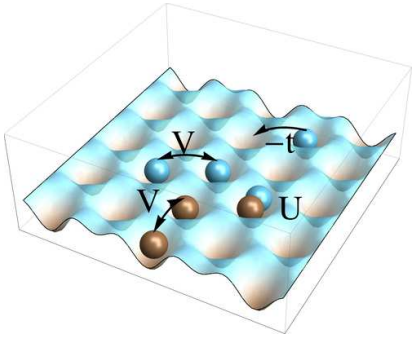

FIG. 1: Triangular lattice hosting bosons of two species labelled a (blue) and b (brown). the bosons can hope from two neighboring sites with the energy $-t$, and interact via an intra-species interaction V and a point contact inter-species interaction U.

In this paper, we provide a theoretical study of a two-species bosonic mixture on a triangular lattice as depicted in Fig. 1. We aim to focus on the most simple model with competing interactions in frustrated geometry in order to study possible mechanisms for stabilizing exotic phases. The richness of the phase diagram of a related one-species model with hard core constraint[12] allows us to expect even more exotic physics for a mixture of two mutually interacting species. Even though such interactions can be encountered in cold atom systems[11,12,20] with polarized dipoles[26,31,32], the present work describes the maximally frustrating cases for which all interactions are repulsive. We address the following issues: (i) how on-site and nearest neighbor interactions compete and (ii) how lattice frustration impacts on the stabilization of non-conventional phases of such a mixture.

To achieve these goals, we use mainly a *cluster mean field* theory (CMFT) and exact diagonalizations (ED) on periodic clusters; both methods are detailed, along with the model we consider, in Section II. Note that preliminary Quantum Monte-Carlo (QMC) simulations have been performed to support our findings (see text). We present in Section III an overview of the phase diagram obtained this way, before focusing on the most interesting phases. First, we describe in Section IV some commensurate spin-like phases. These are characterized with means of perturbative approaches; they have frozen densities and, for one of them, spin-like supersolidity. Next, we analyze in Section V incommensurate phases found in this study: these include two original two-species supersolid (SS) phases, which belong to our main findings. Eventually we address in Section VI the nature of phase transitions involving these peculiar phases, before some concluding remarks in Section VII.

II. MODEL AND METHOD

We study a two-species (spin) extended Bose-Hubbard model on a triangular lattice:

$$\begin{aligned} H_\alpha &= \sum_{\langle i,j\rangle}\Big[-t_\alpha(b^\dagger_{i\alpha}b_{j\alpha}+h.c.)+V_\alpha n_{i\alpha}n_{j\alpha}\Big]-\mu_\alpha\sum_i n_{i\alpha} \\ H_{ab} &= \sum_\alpha H_\alpha + U\sum_i n_{ia}n_{ib}. \end{aligned} \quad (1)$$

H_α is the one-species Hamiltonian ($\alpha = a, b$), with t_α and V_α respectively the nearest neighbor hopping and interaction amplitudes; μ_α is the chemical potential for bosons of species α created by operators $b^\dagger_{i\alpha}$ at site i. In this work, we focus on the limit of hard core bosons ($U_{\alpha,\alpha} \gg |t_\alpha|, V_\alpha, \mu_\alpha$) with an implicit onsite intra-species repulsion $U_{\alpha\alpha}\sum_i n_{i\alpha}(n_{i\alpha}-1)/2$. Together with the repulsive interspecies coupling U, this allows us to maximize the effects of frustration. We have studied the more general case in function of independent μ_a and μ_b and found that the richest physics was found in the symmetric case $\mu_a = \mu_b$, including the novel supersolid regimes. Hence, when the system is (a, b)-symmetric ($t_\alpha = t$, $V_\alpha = V$ and $\mu_\alpha = \mu$), as considered in this work since the most original two-spin phases arise there, the particle-hole transformation $b'_{i\alpha} = b^\dagger_{i\alpha}$ allows for a mapping between $\mu^* > 0$ and $\mu^* < 0$, with $\mu^* = \mu - 3V - U/2$ a rescaled chemical potential. Note that, such a transformation, if restricted to a single species and for $\mu^* = 0$ amounts to changing the sign of U. This $U < 0$ case is of interest since the corresponding terms mimic qualitatively the effects of interlayer short-range interactions in dipolar cold atom bilayers[20].

We compute the ground states of H_{ab} on periodic clusters with up to $N = 12$ sites (see Fig.2), using either CMFT (if not precised) or ED methods. Note that the former method has been employed successfully in many one-species bosonic systems on various lattices such as triangular[12,28,35], pentagonal[33] and hexagonal[2]. It is thus expected to be also very efficient in the present model.

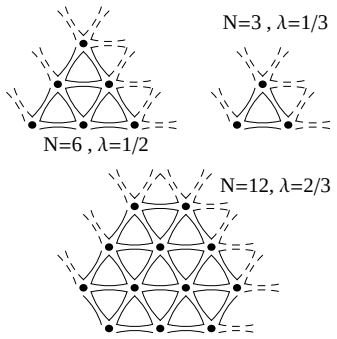

FIG. 2: Clusters considered in our CMFT analysis with $N = 3$, 6 and 12 sites. Internal and external bonds correspond respectively to continuous and dashed lines. For each cluster, the cluster scaling parameter λ is given.

In the former case, the N_i (N_e) internal (external) bonds are treated exactly (at the mean field level)[12,34,35] and correlations are better taken into account as N increases. As in Ref.[35], we thus define the scaling parameter $\lambda = N_i/(3N)$ which quantifies finite boundary effects; the Thermodynamic Limit (TL) is achieved for $\lambda \to 1$ (infinite lattice). The mean-field parameters determined self-consistently are the densities $\bar{n}_{i\alpha} = \langle n_{i\alpha}\rangle$ and the superfluid fractions (SF) $\phi_{i\alpha} = \langle b_{i\alpha}\rangle$. In addition, to evidence 3-fold symmetry breaking, we define the order parameter $M_\alpha = |\bar{n}_\alpha(k)|$, the diagonal $S^d_{ab} = |\langle(n_a - n_b)(-k)(n_a - n_b)(k)\rangle|$ and off-diagonal $S^{od}_{ab} = |\langle\sum_{i,j} b_{ia}b^\dagger_{ib}b_{jb}b^\dagger_{ja}\rangle|/N^2$ correlation functions. We used the Fourier transform $n_\alpha(k) = \frac{1}{N}\sum_s n_{s\alpha}e^{ik\cdot r_s}$ at point $k = (4\pi/3, 0)$, corner of the Brillouin zone.

III. OVERVIEW OF THE PHASE DIAGRAM

Let us first focus on the (μ^*, U) phase diagram in which two-species phases - detailed along the paper - emerge, illustrated here for $t/V = 0.15$. For these parameters, the one-species Hamiltonian H_α is known to present a rich phase diagram with either empty/full, homogeneous superfluid, $\sqrt{3}\times\sqrt{3}$ solid at density 1/3 or 2/3, or supersolid phases[11]. When U is switched on, the correlations between the two species increase, and the resulting GS can be either a product of two one-species phases or a species-entangled state as depicted in the phase diagram shown in Fig. 3. (i) As $\mu^* < 0$ increases, the first non-trivial phase encountered is a homogeneous two-spin superfluid with $\phi_a = \phi_b \neq 0$ ($\phi_\alpha = \frac{1}{N}\sum_i \phi_{i\alpha}$). When n_a and n_b are large enough, V and U terms drive the system into a 3-fold ordered insulator characterized by $\phi_a = \phi_b = 0$ and a total density $n = 2/3$ ($n_a = n_b = 1/3$), the two-species counterpart of the $\sqrt{3} \times \sqrt{3}$ phase. (ii) At even larger

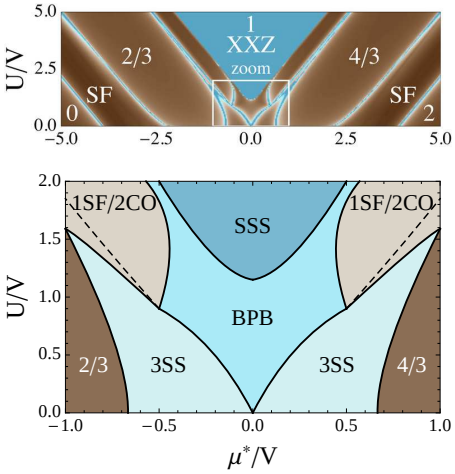

FIG. 3: Phase diagrams as obtained from CMFT calculations on a $N = 3$ cluster at $t = 0.15$ and $V = 1$. Top: wide range of μ^* showing two-spin superfluids, 2/3 and 4/3 plateaus, XXZ physics domain and original collective two-spin physics (white rectangle). Bottom: zoom of the white rectangle and all new two-spin phases (see text for acronyms). Solid (dashed) lines are phase boundaries subsisting (vanishing) in the Thermodynamic Limit (TL).

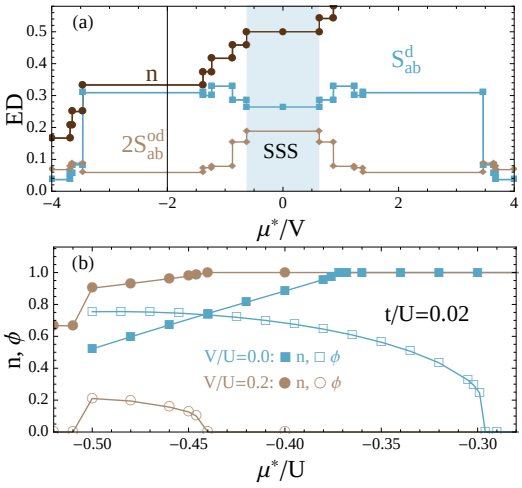

FIG. 4: Strong U regime characterized using either $N = 12$ (ED: a) or $N = 6$ (CMFT: b) clusters. (a) n, S^d_{ab} and S^{od}_{ab} as a function of μ^*/V for $U = 2V$ and $t = 0.15V$. The $n = 1$ plateau and both finite S^d_{ab} and S^{od}_{ab} evidence the SSS; (b) n and $\phi = \phi_a + \phi_b$ as a function of μ^*/U distinguishing the SSF ($V = 0$) and the SSS ($V = 0.2U$) regimes.

density, various supersolids with 3-sublattice structures are stabilized; they will be discussed in detail in Section V. Finally, an insulating regime with $n = 1$ is stabilized for $U > 1.2V$ in the vicinity of $\mu^* = 0$; it will be the object of Section IV. For $\mu^* > 0$, we obtain an equivalent phase diagram thanks to the particle-hole symmetry.

IV. COMMENSURATE SPIN-LIKE PHASES

For strong inter-species repulsion $U \gg V, t, |\mu^*|$ (triangular uppermost domain on Fig. 3-up) the system is Mott insulating, with $\phi_\alpha = 0$ and $n = 1$. Indeed, U imposes the local constraint of single occupancy defined as $\bar{n}_{ia} + \bar{n}_{ib} = 1$. This is reflected by $n = 1$ plateaus in both ED (Fig. 4-a) and CMFT (Figs. 4-b and 7) results. In order to better describe this regime, we define spin 1/2 operators $\sigma^z_i = (n_{ia} - n_{ib})/2$ and $\sigma^+_i = b^\dagger_{ia} b_{ib}$. At second order of the perturbation theory, we obtain an effective XXZ model

$$H_{\rm XXZ} = -\frac{J_\perp}{2} \sum_{\langle i,j \rangle} (\sigma^+_i \sigma^-_j + \sigma^-_i \sigma^+_j) + J_z \sum_{\langle i,j \rangle} \sigma^z_i \sigma^z_j, \quad (2)$$

where $J_\perp = 4t^2/U$ and $J_z = 2V + 4t^2/U$.

Interestingly, this model predicts a $(2m_z, -m_z, -m_z)$ SS with diagonal $\langle \sigma^z \rangle \neq 0$ and off-diagonal $\langle \sigma^+ \rangle \neq 0$ order parameters when $J_z/J_\perp > 4.6(1)$; otherwise, a SF with only off-diagonal order[36,37]. In the present context, these phases correspond respectively to a *spin supersolid* (SSS) and a *spin superfluid* (SSF). While the density is uniform, the SSS has a $(2m_z, -m_z, -m_z)$ structure where m_z quantifies the *spin* disproportion on each sublattice. As depicted in Fig. 4 and Fig. 5(a), for $|\mu^*| \ll V, U$, both ED and CMFT approaches confirm the existence of the SSS; indeed the finite structure factors S^d_{ab}, S^{od}_{ab} and $M = (M_a + M_b)/2$ for $t/U < 0.17$ signal long-range correlations and the corresponding XXZ couplings verify $J_z/J_\perp = 1 + UV/2t^2 \geq 20.5$. In contrast, for $V = 0$ and $t/U \leq (t/U)_c \simeq 0.05(1)$ we find in vicinity of $\mu^* = 0$ the spatially uniform SSF predicted in the XXZ model, as illustrated in Fig. 4(b). Finally, Fig. 5(b) shows that the kinetic energy gain $\epsilon^* \simeq -kt^2/U$ w.r.t. the electrostatic contribution $N(V - \mu)$ is well reproduced by the XXZ model in both regimes; this validates our approach.

V. INCOMMENSURATE SUPERSOLIDS

In contrast to the above mentioned SSS in which supersolidity comes from the species (spin-like) degrees of freedom, in SS phases discussed here n_α may be incommensurate and have finite ϕ_α. From the species-resolved observables shown in Fig. 6 and 7, we identify three such SS phases. (i) For large $U/V = 2$ (right column) and μ^*/V about $\pm 1.0(2)$, the finite M_α indicates a 3-fold order (3FO for both species, while only one species has a non-zero ϕ_α. This phase, dubbed 1SF/2CO in Fig. 3, is a rearrangement of two one-species phases of H_α, the $\sqrt{3} \times \sqrt{3}$ solid and the SS obtained from it by enhancing the quantum fluctuations[11,12]. Two sublattices are (almost) filled by a and b bosons respectively, while on the remaining, an incommensurate density for bosons of one species (*e.g.* a) accounts for superfluidity ($\phi_a > 0$) and a population imbalance ($n_a > n_b$). Within this structure,

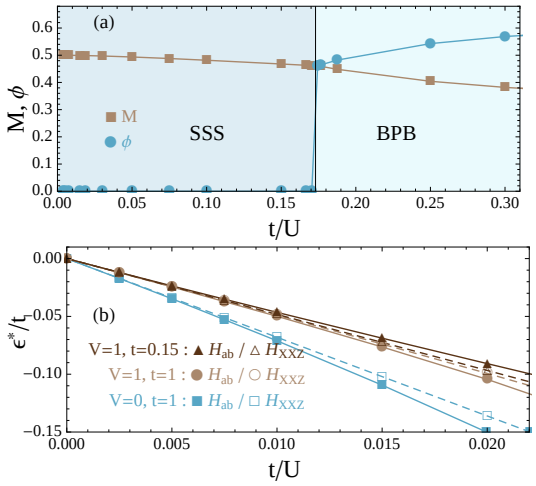

FIG. 5: Strong U regime characterized using either $N = 6$ (CMFT: a) or $N = 12$ (ED: b) clusters. (a) Species-averaged order parameter M and superfluid fraction Φ, evidencing the quantum fluctuation enhancement from the SSS to the BPB phase at $V = 1$ and $t = 0.15$; (b) comparison of the kinetic energy gain $\epsilon^* \simeq -kt^2/U$ for H_{ab} (filled) and $H_{\rm XXZ}$ (empty) for three (t, V) sets.

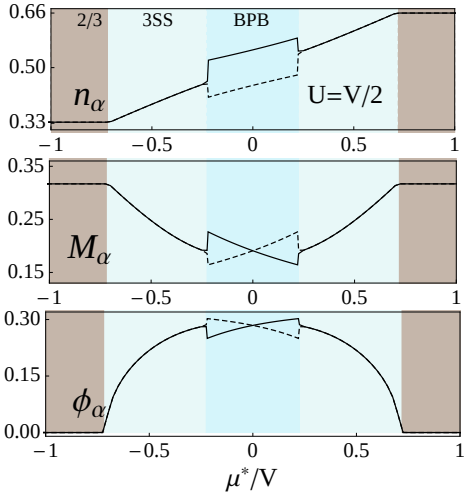

FIG. 6: Species-resolved observables $(n_\alpha, M_\alpha, \phi_\alpha)$. Each species corresponds to either continuous or dashed line. All data come from a $N = 6$ CMFT with fixed $t/V = 0.15$ and $U = 0.5V$. The arrow points out a tiny region which disappears in the TL (see text). The shaded regions correspond to the different phases of Fig. 3.

the repulsion energy $\propto U$ is minimized thanks to the localization of bosons of a single species. (ii) A distinct phase is found for small $U/V = 0.5$ (left column) and μ^*/V about $\pm 0.5(3)$, with a finite ϕ_α for both species as well as a 3-fold symmetry breaking.

As shown in the typical snapshot obtained by CMFT in Fig. 8(c), it can be seen as a superposition of two one-species SS (these would be obtained at $U = 0$); both

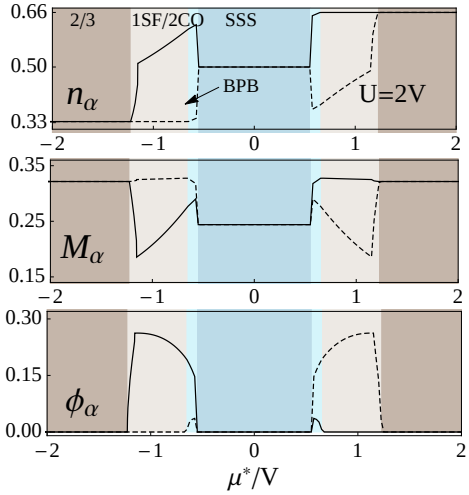

FIG. 7: Same as Fig. 6, but for $U = 2V$.

species contribute symmetrically to superfluidity. This phase, called 3-fold SS (3SS) is the first example of a collective two-species supersolid and is obtained from the parent $n = 2/3$ solid by a defect condensation upon doping as μ^* increases. As in this parent state, the weak

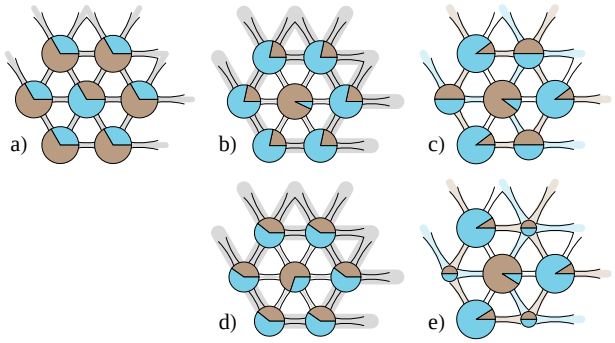

FIG. 8: Examples of two-spin supersolids with 3-sublattice structure obtained by CMFT density maps on the 12-site cluster (a,b,c) and by QMC correlations for 36×36 sites cluster (d,e). (a) the $n = 1$ *spin* supersolid (SSS) at $\mu^* = 0$ and $U = 2V$; (b) and (c) respectively the bosonic pinball (BPB) at $\mu^* = -0.15V$ and the 3-supersolid (3SS) at $\mu^* = -0.25V$, for $t = 0.15V$ and $U = 0.5V$. $n_a - n_b$ is 0 for the 3SS and finite for the BPB for all CMFT clusters (Fig. 9 for the TL study). (d) and (e) are respectively QMC results for the BPB at $\mu^* = -0.12V$ and the 3SS at $-0.72V$. Note that the 3SS and BPB have distinct symmetries (under $\pi/6$ rotations).

inter-species coupling merely forces the localized a and b bosons to occupy distinct sublattices. (iii) The most remarkable incommensurate SS phase is achieved, upon increasing t/U, when quantum fluctuations become too strong for the density-uniform $n = 1$ SSS phase. This original two-species SS is called the *bosonic pinball* (BPB) due to a structure very similar to its fermionic coun-

terpart with similar interactions, the *pinball liquid*, and is depicted in Fig. 8(b,d). The latter has almost one localized electron per site on one sublattice (pins) and a metallic behavior on the remaining hexagonal lattice (balls)[28,29,38]. Here, the particles are bosonic and the species play the role of the spins. The structure is depicted on Fig.1(b). One sublattice, forming a triangular super-lattice with $\bar{n}_{ia}+\bar{n}_{ib}$ close to 1, is filled in majority by one type of bosons. The two-spin superfluid character is carried by the remaining bosons on the complementary hexagonal lattice. This is shown in the BPB region on Fig. 6 and Fig. 9, by a coexistence of solid ($M_\alpha \neq 0$) and superfluid ($\phi_\alpha \neq 0$) orders in both species. This lattice symmetry breaking is reminiscent of the parent SSS phase, the partial quantum melting of which involves a condensation of two types of defects coming from doubly-occupied and empty sites. Finally, unlike the 3SS and 1SF/2CO, the BPB can be stabilized at the $n = 1$ commensurability when $\mu^* = 0$.

VI. THERMODYNAMIC LIMITS AND PHASE TRANSITIONS

All the phases described above exist in the TL. Indeed, in Fig. 9 are evidenced the cluster dependencies of M and ϕ, shown as functions of μ^* and the examples of the BPB and the 3SS (c) prove their finiteness as $\lambda \to 1$. We also checked that the phase diagram is only weakly

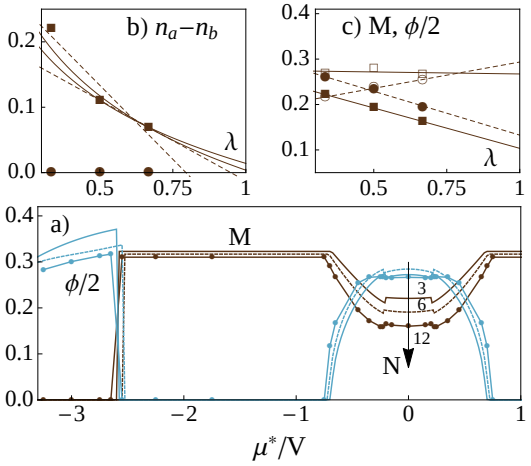

FIG. 9: M and ϕ as a function of μ^* for $t = 0.15V$ and $U = 0.5V$ obtained by CMFT on clusters of $N = 3$ (continuous), 6 (dashed) and 12 (symbols) site. See Fig. 2 for the cluster shapes. Cluster scalings as function of λ (see text) are shown for b) $n_a - n_b$ with different possible fits giving either zero (continuous) or finite (dashed) TL values (see text) and c) M (filled symbols) and $\phi/2$ (empty symbols) within both the BPB at $|\mu^*| = t$ (squares) and the 3SS at $|\mu^*| = 3t$ (circles).

affected by size effects thus Fig. 3 is representative of the TL. In the strong correlation limit $U, V \gg t$ [39], perturbation theory allows to locate phase transitions where the defect energy vanishes (condensation), *e.g.* for the $2/3 \to$ 3SS transition. Consider a defect consisting of an extra boson (say of species a) inserted in the *empty* sublattice of the 2/3 crystal with the energy cost $3V$. Via second order processes, such a defect can hop to second neighbors with an amplitude $-t_{\rm eff} = -t^2/U - t^2/V$. The terms $-t^2/U$ and $-t^2/V$ account respectively for processes where (i) the extra a boson hops via the b-filled sublattice, or (ii) a vacancy on the a-filled sublattice is created and then deleted. In this limit, the defects condense and lead to supersolidity for $\mu_c = 3V - 6t_{\rm eff}$, *e.g.* $\mu_c/V \simeq -0.65$ for $U = 0.5V$ in good agreement with the results of Fig. 6 and 7. This defect condensation mechanism implies a gauge symmetry breaking, additionally to the lattice symmetries already broken in the 2/3 phase. This indicates that the transition is of second order, as confirmed by the absence of discontinuities in ϕ and M as function of μ (Fig. 9). This corresponds to the standard picture of defect condensation accounting for an incommensurate SS; the SF density (here inhomogeneous) is carried by defects on top of density modulations[11]. In contrast, the transitions between (i) homogeneous SF and 2/3 solid, and (ii) the BPB and 3SS are found of first order, characterized by hysteresis in the CMFT. We find distinct transition points if μ is, from one CMF calculation to another, either stepwise increased or stepwise decreased (see [40]). In case (ii), $n_a - n_b$ (Fig. 9(b)) has distinct size-dependence, but a vanishing value in the TL cannot be ruled out for the BPB, despite a non-linear behavior. $n_a - n_b$ is strictly 0 for the 3SS. For the BPB, the non-linear behavior makes difficult to extract $n_a - n_b$ as $\lambda \to 1$, and various fits can give either zero (linear) or finite (*e.g.* weighted $a + \lambda^b$) value. However, BPB and 3SS have different symmetries as obtained by CMFT (Fig. 8(b,c)) and confirmed by preliminary QMC calculations. Indeed, to check this point, we have performed Stochastic Series Exchange (SSE) QMC simulations on clusters up to 36×36 sites for various U in function of μ^*, for which real-space correlations $\langle n_{sa} n_{i\alpha}\rangle$(for site i far away from the reference site s to get rid of short-distance effects) confirm the existence and symmetries of both the 3SS and the BPB (Fig. 8(d,e)). The complete analysis of this model by SSE-QMC, being beyond the scope of this paper, will constitute a separate work.

VII. CONCLUSION

We study an interacting two-species bosonic mixture on a triangular lattice by combining CMFT, ED and perturbative methods, supported by SSE-QMC results. We focus on a region of parameter space in which peculiar phases arise due to the competition between frustration and quantum fluctuations. Within a very rich and complex phase diagram, we evidence three original mixture supersolids, a commensurate *spin supersolid* (SSS) and two mutually competing incommensurate phases arising from the partial quantum melting of parent states. The

most interesting phase, dubbed *bosonic pinball* (BPB) due to an inner structure very reminiscent of its fermionic counterpart[29], results from strong inter-species effects. It is worth mentioning that this rich physics is found for attractive U (for specific parameters), a situation more directly connected to dipolar cold atom bilayer experiments. We hope this work will stimulate further investigations in this direction.

Acknowledgments

A.R. and F.T. acknowledge financial support by the Agence Nationale de la Recherche under grant No. ANR 2010 BLANC 0406-0. P.R.-F. would like to thank Néel Institute for kind hospitality.

[1] D. Jaksch, C. Bruder, J. I. Cirac, C. W. Gardiner, and P. Zoller, Phys. Rev. Lett. **81**, 3108 (1998).
[2] A. F. Albuquerque, D. Schwandt, B. Hetényi, S. Capponi, M. Mambrini, and A. M. Läuchli, Phys. Rev. B **84**, 024406 (2011).
[3] A. Ralko, F. Becca and, D. Poilblanc, Phys. Rev. Lett. **101** 117204 (2008).
[4] M. V. Feigelman, V. B. Geshkenbein, L. B. Ioffe, and A. I. Larkin, Phys. Rev. B 48, 16641 (1993).
[5] D. Das and S. Doniach, Phys. Rev. B 60, 1261 (1999).
[6] A. Paramekanti, L. Balents, and M. P. A. Fisher, Phys. Rev. B 66, 054526 (2002).
[7] A. Ralko, F. Trousselet and, D. Poilblanc, Phys. Rev. Lett. **104** 127203 (2010).
[8] E. Kim and M. H. W. Chan, Nature **427**, 225 (2004).
[9] N. Prokof'ev and B. Svistunov, Phys. Rev. Lett. **94**, 155302 (2005).
[10] B. Capogrosso-Sansone, C. Trefzger, M. Lewenstein, P. Zoller, and G. Pupillo, Phys. Rev. Lett. **104**, 125301 (2010).
[11] S. Wessel and M. Troyer, Phys. Rev. Lett. **95**, 127205 (2005); D. Heidarian and K. Damle, Phys. Rev. Lett. **95**, 127206 (2005); R. G. Melko, A. Paramekanti, A. A. Burkov, A. Vishwanath, D. N. Sheng, and L. Balents, Phys. Rev. Lett. **95**, 127207 (2005).
[12] S. R. Hassan, L. de Medici, and A. M. S. Tremblay, Phys. Rev. B **76**, 144420 (2007).
[13] L. Pollet, J.D. Picon, H.P. Büchler, and M. Troyer, Phys. Rev. Lett. **104**, 125302 (2010).
[14] D. Y. Kim and M. H. W. Chan, Phys. Rev. Lett. **109**, 155301 (2012).
[15] P. Sengupta, L. P. Pryadko, F. Alet, M. Troyer, and G. Schmid, Phys. Rev. Lett. **94**, 207202 (2005).
[16] C. Becker, P. Soltan-Panahi, J. Kronjäger, S. Dörscher, K. Bongs, and K. Sengstock, New J. Phys. **12**, 065025 (2010).
[17] G.-B. Jo, J. Guzman, C. K. Thomas, P. Hosur, A. Vishwanath, and D. M. Stamper-Kurn, Phys. Rev. Lett. **108**, 045305 (2012).
[18] J. Catani, L. DeSarlo, G. Barontini, F. Minardi, and M. Inguscio, Phys. Rev. A **77**, 011603 (2008).
[19] B. Gadway, D. Pertot, R. Reimann, and D. Schneble, Phys. Rev. Lett. **105**, 045303 (2010).
[20] C. Trefzger, C. Menotti and M. Lewenstein, Phys. Rev. Lett. **103**, 035304 (2009).
[21] P. Buonsante, S. M. Giampaolo, F. Illuminati, V. Penna, and A. Vezzani, Phys. Rev. Lett. **100**, 240402 (2008); A. Argüelles and L. Santos, Phys. Rev. A **75**, 053613 (2007); T. Roscilde, C. Degli Esposti Boschi, M. Dalmonte, EPL **97**, 23002 (2012).
[22] L. de Forges de Parny, F. Hébert, V. G. Rousseau, R. T. Scalettar, and G. G. Batrouni, Phys. Rev. B **84**, 064529 (2011); K. Hettiarachchilage, V. G. Rousseau, K.-M. Tam, M. Jarrell and J. Moreno, arXiv:1212.4478.
[23] Also Bose-Fermi mixtures have been considered on the triangular lattice: L. Mathey, S. W. Tsai, and A. H. Castro Neto, Phys. Rev. B **75**, 174516 (2007); P. P. Orth, D. L. Bergman and K. Le Hur, Phys. Rev. A **80**, 023624 (2009).
[24] L. He, Y. Li, E. Altman, and W. Hofstetter, Phys. Rev. A **86**, 043620 (2012).
[25] Y. Kuno, K. Kataoka, and I. Ichinose, Phys. Rev. B **87**, 014518 (2013).
[26] T. Lahaye et al., Rep. Prog. Phys. **72**, 126401 (2009), H. P. Büchler, E. Demler, M. Lukin, A. Micheli, N. Prokofev, G. Pupillo and P. Zoller, Phys. Rev. Lett. **98**, 060404 (2007).
[27] B. Capogrosso-Sansone, Ş. G. Söyler, N. V. Prokof'ev, and B. V. Svistunov, Phys. Rev. A **81**, 053622 (2010).
[28] L. Cano-Cortés, J. Merino and S. Fratini, Phys. Rev. Lett. **105**, 036405 (2010); L. Cano-Cortés, A. Ralko, C. Février, J. Merino, and S. Fratini, Phys. Rev. B **84**, 155115 (2011).
[29] J. Merino, A. Ralko, and S. Fratini, Phys. Rev. Lett. **111**, 126403 (2013).
[30] O. Tieleman, A. Lazarides, and C. Morais Smith, Phys. Rev. A **83**, 013627 (2011).
[31] R. M. Lutchyn, E. Rossi, and S. Das Sarma, Phys. Rev. A 82, 061604(R) (2010).
[32] J. R. Armstrong, N. T. Zinner, D. V. Fedorov, and A. S. Jensen, Eur. Phys. J. D. **66**, 85 (2012).
[33] A. Ralko, Phys. Rev. B **84**, 184434 (2011).
[34] E. Zhao and A. Paramekanti, Phys. Rev. B **76**, 195101 (2007).
[35] D. Yamamoto and I. Danshita, Phys. Rev. B **88**, 014419 (2013).
[36] D. Heidarian and A. Paramekanti, Phys. Rev. Lett. **104**, 015301 (2010).
[37] A. Sen, P. Dutt, K. Damle and R. Moessner, Phys. Rev. Lett. **100**, 147204 (2008).
[38] C. Hotta and N. Furukawa, Phys. Rev. B **74**, 193107 (2006).
[39] X. F. Zhang, R. Dillenschneider, Y. Yu, and S. Eggert, Phys. Rev. B **84**, 174515 (2011).
[40] D. Yamamoto, I. Danshita, and C. A. R. Sà de Melo, Phys. Rev. A **85**, 021601 (2012).